The metal-binding domain of IGFBP-3 selectively delivers therapeutic molecules into cancer cells

Anja Huq[a,b], Baljit Singh[a,b], Thea Meeker[b] and Desmond Mascarenhas[a,b]

Conventional chemotherapy for cancer has limited specificity for cancer cells. Here, we investigate the possibility of improving the selectivity of chemotherapy by coadministering targeted biological modifier peptides. We show that the 22-amino acid metal-binding transporter domain (MBD) derived from insulin-like growth factor-binding protein-3 selectively targets cancer cells. The rate of MBD uptake by cells was measured using a panel of 54 human cancer cell lines and correlated with MBD cross-linking to cell surface transferrin receptor, caveolin 1, and integrin β. Gene array data show that MBD uptake correlates with the expression of genes associated with cellular stress-coping mechanisms commonly upregulated in cancer (nuclear factor-κB, Hsp-70B). MBD-tagged peptides designed to inhibit such mechanisms have cytotoxic effects on a broad range of human cancer cell lines. The discriminant validity of these peptides as potential cotherapeutic agents was investigated by comparing their cytotoxicity to cancer cell lines versus normal human cell counterparts. Synergies between these peptides and marginally cytotoxic levels of 5-fluorouracil were demonstrated. Biodistribution data from in-vivo experiments in mice and rats confirm that MBD-tagged peptides and proteins preferably localize to specific tissues, such as kidney and pancreas. Intracardial injection of CCRF-CEM T-cell leukemia or MDA-MB-435 cells into Rag-2 mice establishes disseminated disease within 7 days. Twenty-five-day subcutaneous administration of a three-peptide cocktail (3 mg/kg) in combination with 5-fluorouracil in Rag-2 mice with established CCRF-CEM leukemia significantly reduces splenomegaly and bone marrow cancer cell burden. In a similar experiment using MDA-MB-435 cells, MBD-tagged peptides reduced human cell burden in bone marrow. Taken together, these data suggest that MBD-tagged molecules can be used as highly selective chemosensitizers in the treatment of hematological and disseminated malignancies. *Anti-Cancer Drugs* 20:21–31 © 2009 Wolters Kluwer Health | Lippincott Williams & Wilkins.

Anti-Cancer Drugs 2009, **20**:21–31

Keywords: biological modifiers, chemosensitizer, 5-fluorouracil insulin-like growth factor-binding protein-3, mechanistic specificity, metal-binding domain, metastasis, peptide therapeutic, systemic disease

[a]Mayflower Organization for Research and Education and [b]Protigen Inc., Sunnyvale, California, USA

Correspondence to Dr Desmond Mascarenhas, PhD, Mayflower Organization for Research and Education, 525 Del Rey Avenue, Suite B, Sunnyvale, CA 94085, USA
Tel: +1 408 523 6279; fax: +1 408 523 6261;
e-mail: desmond@mayflowerworld.org

Received 14 June 2008 **Revised form accepted** 10 August 2008

Introduction

Conventional interventions for cancer focus on the use of systemic chemotherapeutic and biological agents to treat disseminated disease, but these treatments almost always lose effectiveness over time. Systemic adjuvant therapy has been studied in more than 400 randomized clinical trials, and has proven to reduce rates of recurrence and death more than 15 years after treatment [1–3]. Owing to limited specificity and high toxicity, however, such treatments significantly lower the patient's quality of life. The same studies have also shown that combinations of drugs are more effective than single drug treatments. Reducing cancer cell burden requires management of cancer cell populations by maximization of spectrum as well as therapeutic index. Future approaches to the treatment of cancer might address the heterogeneity of cancer cell populations by simultaneously targeting multiple hallmarks of the disease: dysregulated growth rates, enhanced survival (from upregulated stress-coping and anti-apoptotic mechanisms), and migration to immunologically privileged sites such as spleen and bone marrow. One logical approach would be to combine (a) selective transportation of therapeutics to privileged sites; (b) selective uptake of the therapeutics by the cancer cells; (c) mechanistic selectivity inside cancer cells; and (d) synergies with other adjuvant therapies.

Global comparison of cancer cells to their normal cell counterparts reveals underlying mechanistic distinctions. Cancer cells display upregulated stress-coping and antiapoptotic mechanisms to successfully evade cell death [4–6]. Many tumor types contain high concentrations of heat-shock proteins (HSPs) of the HSP27, HSP70, and HSP90 families compared with adjacent normal tissues [7–11]. The role of HSPs in tumor development may be related to their function in the development of tolerance to stress [12], and high levels of HSP expression seem to be a factor in tumor pathogenesis. Among other mechanisms individual HSPs can block pathways of apoptosis [13]. Studies show that HSP70 is required for the survival of cancer cells [1]. Stress can also activate the nuclear factor κB (NF-κB)

0959-4973 © 2009 Wolters Kluwer Health | Lippincott Williams & Wilkins DOI: 10.1097/CAD.0b013e3283144610

transcription factor family. NF-κB is a central regulator of the inflammation response. NF-κB, however, regulates the expression of antiapoptotic genes such as those coding for cyclooxygenases and metalloproteinases, thereby favoring tumor cell proliferation and dissemination. Data show that NF-κB can be successfully inhibited by peptides interfering with its intracellular transport and/or stability [14,15]. Human survivin, an inhibitor of apoptosis, is highly expressed in various tumors [16] aberrantly prolonging cell viability and contributing to cancer. It has been shown that ectopic expression of survivin can protect cells against apoptosis [17]. Tumor suppressor p53 is a transcription factor that induces growth arrest and/or apoptosis in response to cellular stress. Peptides modeled on the MDM2-binding pocket of p53 can inhibit the negative feedback of MDM2 on p53 commonly observed in cancer cells [18,19]. Thus, inhibitors selectively targeting stress-coping and antiapoptotic mechanisms might be expected to be disproportionately cytotoxic to cancer cells.

We previously showed that a C-terminal metal-binding domain (MBD) of insulin-like growth factor-binding protein-3 (IGFBP-3) rapidly mobilizes large proteins from the extracellular milieu into the nuclei of target cells [20]. Here, we extend these observations to show that MBD can mediate transport of linked molecules to tissues such as spleen and bone marrow *in vivo*.

Materials and methods

MBD-tagged proteins and peptides and mutant MBD peptide synthesis

MBD-tagged proteins were described previously [20]. The 22-amino acid C-terminal MBD of IGFBP-3 has been used to create a series of peptides by chemical synthesis (Genemed Inc., S. San Francisco, California, USA). The sequences of these peptides are shown in Table 1. Variant collections of MBD peptides were synthesized in 96-well format by Pepscan Systems (Holland) and tested for enhanced cytotoxicity *in vitro*.

Gene arrays

Gene array experiments were performed by Miltenyi Biotec (Auburn, California, USA). Cell pellets from six anatomically matched pairs of high-MBD-uptake and low-MBD-uptake cell lines (DU145, HCT15, HOP62, UO31, OVCAR5, Hs578T, PC3, HAT29, NCI-H23, A498, OVCAR8, and MCF7) were shipped on dry ice and total RNA was isolated using NucleoSpin RNA II. Total RNA of 1 μg was used for linear amplification (PIQOR manufacturer's manual) and amplified RNA underwent a quality control check with the Bioanalyzer 2100 system. Amplified RNAs were fluorescently labeled and the fluorescently labeled probes were subsequently hybridized on customized PIQOR Microarrays (Miltenyi Biotech). SAM (Significance Analysis of Microarrays; Tusher *et al.*, 2001) was carried out to identify those genes, which might be correlated with MBD uptake (either upregulated or downregulated). Data analysis was conducted by taking the streptavidin–horseradish peroxidase complex (SAHRP) uptake rates for the 12 cell lines (Table 1) and correlating them to the gene expression levels of approximately 1000 genes on the array. Genes showing an r^2 value of greater than 0.1 and averaged (six pairs) up ($> 1.5\times$) or down ($< 0.75\times$) gene expression levels are listed in Table 3 and one of these, GDF-15, was selected for further analysis.

Cells

All cell lines were obtained from Cambrex (E. Rutherford, New Jersey, USA) or the American Type Culture Collection. Breast cancer cell lines (MCF7, MDA-MB-435, MDA-MB-231, MX-1), leukemia cell lines (RPMI-8226, CCRF-CEM, MOLT-4), and prostate cancer cell lines (PC3, DU145, LNCAP) were cultured in RPMI-1640 media supplemented with 5% fetal bovine serum (FBS). Paired noncancer and breast cancer cell lines (CRL-7481/CRL-7482, CRL-7364/CRL-7365) were cultured in Dulbecco's modified Eagle's medium supplemented with 10% FBS. Normal breast cell lines MCF-10A, HMEC-mammary epithelial cells, and HTB-125 are cultured in specialized media [MCF10A and HMEC need MEGM Bullet Kit media (Clonetics) and HTB-125 needs Hybri-Care Media (American Type Culture Collection) supplemented with 30 ng/ml EGF and 10% FBS].

Animal models

All animal studies were performed according to IACUUC approved protocols. A previously described Rag2/gC murine model [21] of human leukemia was used. Mice (Taconic, Seattle, Washington, USA) were bred by crossing C57BL/6J gc knockout mice to C57BL/10SgSnAi Rag-2 deficient mice. On the basis of preliminary studies using well-characterized HL60 cells, we selected C57BL/Rag-2/gC mice for MBD-peptide tests. First, we confirmed successful establishment of leukemia in Rag-2 mice using intracardial injection. CCRF-CEM or MDA-MB-435 xenograft-bearing Rag-2 mice (approximately 5×10^5 cancer cells injected per animal per group; six to 10 animals per group) were established through intracardial injection. MBD peptides were injected once daily into the animals by subcutaneous bolus (0.2–1.0 mg/kg each peptide). Blood sampling and PCR analysis were carried out at weekly intervals. Approximately 100 μl of blood was collected from the saphenous vein. PCR analysis was performed on peripheral blood (PB) on day 3 postinjection to determine whether animals had successfully established leukemia/cancer. Cancer cell count levels were monitored during and after the treatment as well as at termination. PCR analysis on PB, bone marrow, spleen, liver, and lung is used to quantify the cancer cells. At day 3, before treatment, high levels of cancer cells were invariably seen in PB and low

Table 1 MBD-mediated uptake of streptavidin–horseradish peroxidase into cancer cells

		MBD-mediated uptake of SAHRP[a]			
		MBD9		MBD21	
Cell line	Histologic type	Cytoplasmic	Nuclear	Cytoplasmic	Nuclear
SK-0V-3	hu Ascites adenocarcinoma	2.0	0.4	<0.04	<0.04
OVCAR-3	hu Ascites adenocarcinoma	2.4	4.6	<0.04	3.2
HOP 92	hu Lung large cell, undifferentiated	2.5	1.6	1.5	1.6
NCI-H226	hu Lung sqamous cell	2.6	1.8	0.7	0.9
K562	Lymph leukemia	2.6	1.3	2.8	1.1
CCRF-SB	Lymph leukemia	2.6	0.6	1.7	0.1
OVCAR-5	hu Adenocarcinoma	2.7	1.2	1.3	1.5
786-O	hu Renal adenocarcinoma	2.9	3.9	1.8	4.8
COLO 205	hu Ascitic fluid adenocarcinoma	2.9	0.9	2.1	0.9
DU-145	hu Prostate carcinoma	3.1	<0.04	25.7	3.3
SW-620	hu Colon adenocarcinoma	3.2	0.7	6.3	2.3
WIDR	hu Colon adenoarcinoma	3.4	0.7	2.8	1.0
HS 913T	hu Lung mixed cell	3.4	1.1	2.1	1.8
KM12	hu Adenocarcinoma	3.6	1.0	2.1	0.7
OVCAR-8	hu Adenocarcinoma	3.9	5.0	6.1	13.1
HCT-15	hu Colon adenocarcinoma	4.0	0.8	2.7	0.7
TK-10	hu Renal carcinoma	4.0	1.3	5.0	2.2
UO-31	hu Renal carcinoma	4.6	1.0	1.3	3.3
HCC 2998	hu Adenocarcinoma	4.6	3.7	2.1	2.4
NHI-H322M	hu Lung bronchi alveolar carcinoma	5.2	5.0	6.0	8.3
HT-29	hu Recto-sigmoid colon adenocarcinoma	6.1	7.7	3.5	9.5
RPMI 8226	Lymph leukemia	6.5	0.0	3.6	0.0
HS-578T	hu Ductal carcinoma	6.8	2.3	2.8	2.3
IGR-OV1	hu R ovary cysto adenocarcinoma	7.0	2.6	1.9	1.0
BT-549	hu Lymph node infil. Ductal carcinoma	7.2	2.1	4.8	3.3
EKVX	hu Lung adenocarcinoma	7.2	4.2	7.7	7.3
CAKI-1	hu Renal adenocarcinoma	7.4	1.8	2.8	1.0
Lewis Lung	hu Lung carcinoma	8.6	7.2	6.4	3.4
435	Breast adenocarcinoma	8.6	2.7	6.1	1.3
NCI-H522	hu Lung adenocarcinoma	9.1	3.7	5.1	1.7
A549	hu Lung adenocarcinoma	9.6	3.5	4.4	1.3
ACHN	hu Renal carcinoma	9.6	2.9	8.0	3.1
231	Breast adenocarcinoma	9.6	2.6	3.4	1.1
OVCAR-4	hu Adenocarcinoma	9.9	2.7	6.1	1.3
SN12C	hu Renal carcinoma	10.6	3.5	6.7	6.4
NCI-H23	hu Lung adenocarcinoma	10.8	6.6	8.0	8.7
MX-1	hu Breast mammary carcinoma	10.8	3.1	8.5	3.8
A704	hu Renal adenocarcinoma	10.9	1.8	4.5	1.2
COLON 26	Carcinoma	11.3	2.3	8.9	2.2
HOP 62	hu Lung adenocarcinoma	12.0	0.9	4.1	0.2
LOVO	hu Colon adenocarcinoma	12.6	5.4	8.7	3.8
MOLT4	Lymph leukemia	12.7	0.0	7.3	0.0
SHP-77	hu Lung small-cell carcinoma	12.8	5.9	6.6	2.7
HCT-116	hu Colon carcinoma	14.1	4.4	12.4	9.5
HOP 18	hu Lung large cell	16.6	8.1	10.3	3.1
A2780	hu Ovary adenocarcinoma	20.7	2.8	7.5	1.0
PC-3	hu Prostate carcinoma	23.2	8.5	44.2	13.2
SR	Leukemia	24.4	0.0	20.9	0.0
CHA-59	hu Bone osteosarcoma	24.7	9.7	8.2	2.1
PAN 02	Pancreatic ductal carcinoma	25.8	7.0	9.3	2.2
MCF 7	Breast adenocarcinoma	26.7	19.8	11.1	5.8
A498	hu Renal carcinoma	28.5	12.4	35.3	33.4
NCI-H460	hu Lung large cell carcinoma	30.3	5.6	11.6	5.8
CCRF-CEM	Lymph leukemia	46.2	1.8	41.3	2.0
HEK 293	Kidney	20.2	20.1	13.6	4.5
	Median	7.4	1.8	2.8	1.0

[a]Units are nanograms HRP detected by ELISA in extracts prepared from cells that had been exposed to 1 μg SAHRP–MBD peptide complex for 20 min; uncomplexed SAHRP background was less than 0.04 ng in all experiments.
MBD, metal-binding transporter domain; SAHRP, streptavidin–horseradish peroxidase complex.

or no levels of human cancer cells in peripheral organs. Blood and peripheral organs were collected at termination and stored for further analysis (day 18).

Cytotoxicity assay

Cells were incubated 48 h with MBD peptide. Fresh peptide was added to the plate every 24 h. All assays were performed in quadruplicate. Each experiment was repeated at least twice and most cytotoxicity experiments were carried out over a dozen times each. Promega 96-well Cell Titer Cytotoxicity Assay Kit was used to determine cell survival in breast cancer and leukemia cell lines and their normal cell counterparts. Using increasing doses of peptides (3.125, 6.25, 12.5, and

25.0 μg/ml) and a fixed number of cells (e.g. 10^4) per well, cytotoxicity was measured after a 48-h incubation at 37°C. MBD-domain-only peptides (MBD9 or MBD-SMZ) were used as controls. The 96-well format allows high-throughput data to determine enhanced and synergistic effects on cell-death, that is, comparing cytotoxicity of peptides singly or in various combinations and with low-level 5-fluorouracil (5-FU; IC-20). 5-FU was purchased from Sigma.

Enzyme-linked immunosorbent assays

Each enzyme-linked immunosorbent assay was carried out in triplicate or quadruplicate. All sample measurements were read off the linear part of the standard curve generated for each type of assay and readings were typically at least two to three times below saturation. Blank controls gave readings at least 10–20 times below the typical sample measurement. The relative cytotoxicity performance of peptides upon a reference panel of cell lines was consistent over at least 2 years of experiments. Cells were lysed using cell lysis buffer (Clontech, Palo Alto, California, USA) or phospho-safe extraction reagent (Novagen, Madison, Wisconsin, USA) and lysate dilutions of 1 : 10 or 1 : 20 were loaded in triplicate in a 96-well plate format. Protein contained in the lysate was allowed to attach to MaxiSorp plates with high affinity to molecules with hydrophilic/hydrophobic domains (Nunc-Immuno Microwell 96-well plates, U-Bottom; VWR International, West Chester, Pennsylvania, USA) for 1 h at room temperature. The plates were then incubated for 1 h at room temperature (or overnight at 4°C) in blocking buffer, consisting of 3% BSA in PBS with 0.05% Tween-20. The plates were washed and incubated with the diluted primary antibody for 1 h on the shaker at room temperature. Anti-MBD primary antibody was produced in-house and is used at a 1 : 2500 dilution. The plates were washed and then incubated with horseradish peroxidase-conjugated secondary mouse or rabbit polyclonal antibody at 1 : 3500 dilutions for 45 min at room temperature. Secondary mouse/rabbit polyclonal antibodies were purchased from (Amersham Biosciences, Piscataway, New Jersey, USA, or VWR). The antibody–antigen complex was visualized with tetramethylbenzidine (TMB) liquid substrate system (Sigma, St Louis, Missouri, USA) according to the manufacturer's protocol. Plates were read at 655 nm on the enzyme-linked immunosorbent assay plate reader (Molecular Devices, Sunnyvale, California, USA).

cDNA PCR analysis

All PCR reactions were confirmed in triplicate. On the basis of gene array data, GDF15 was chosen to evaluate biodistribution of peptides representing stress-coping and antiapoptotic mechanisms through PCR. Human cDNA MTC panel I (#636742, Clontech) was tested against GDF15 (forward primer 5′-GGGCAAGAACTC AGGACGG-3′ and reverse primer 5′-TCTGGAGTCT TCGGAGTGCAA-3′). As a control, a 983-bp fragment was amplified using GAPDH primers (5′-TGAAGGTCG GAGTCAACGGATTTGGT and 3′-CATGTGGGCCAT GAGGTCCACCAC). The PCR was performed in a thermal cycler (Perkin Elmer, Waltham, Massachusetts, USA). The optimized PCR conditions are: 28 cycles of 30 s at 96°C, 40 s at 59°C, and 1 min at 72°C. From a 50-μl PCR reaction 15 μl sample was loaded per well on a 1 × TBE and 10% polyacrylamide gel (Lonza, Walkersville, Maryland, USA) and run out at 90 V for 1.5 h. Bands were visualized by using ethidium bromide staining.

Genomic DNA isolation and genomic DNA PCR

At termination of each animal experiment, blood and organs were collected and stored at −80°C. To isolate genomic DNA (gDNA) from blood samples the blood and cell culture DNA kit (Qiagen) was used, and to isolate gDNA from tissue samples the DNaesy tissue kit (Qiagen) was used. gDNA concentrations were established based on spectrophotometer OD_{260} readings. To determine human genomic DNA in each sample, human-specific primers 5′-TAGCAATAATCCCCATCCTCCATA TAT-3′ and 5′-ACTTGTCCAATGATGGTAAAAGG-3′, which amplify a 157-bp portion of the human mitochondrial cytochrome *b* region [22], were used. As these primers do not amplify murine DNA, they can be used to estimate human cell burden in rodent tissues. Template DNA of 100–500 ng was amplified per PCR reaction, depending on type of tissue. Best results were achieved using the KOD hot start PCR kit (Novagen). PCR was performed in a thermal cycler (Perkin Elmer) for 32 or 35 cycles of 30 s at 96°C, 40 s at 59°C, and 1 min at 72°C. The program was modified from Matsuda *et al.* and optimized for genomic DNA isolated from mouse tissue.

Statistical methods

Probability values (*P* values) were computed using Student's *t*-test. Unless otherwise stated, *P* values are expressed relative to saline-treated controls.

Results

Cancer cells are more susceptible to MBD-uptake than normal cells

Nanomolar nuclear and cytoplasmic concentrations of a approximately 90-kDa SAHRP can be rapidly achieved in cell culture by adding 100 ng/ml of MBD-tagged SAHRP to the culture medium [20]. Three matched cancer/noncancer breast cell line pairs were compared in this in-vitro uptake assay (Fig. 1a). In all cases the cancer cell line took up the MBD-tagged complex more efficiently than the normal counterpart.

MBD-mediated SAHRP mobilization into 54 human cancer cell lines

Nuclear concentrations of SAHRP (a ~90-kDa protein complex) in the nanomolar range can be rapidly achieved

Fig. 1

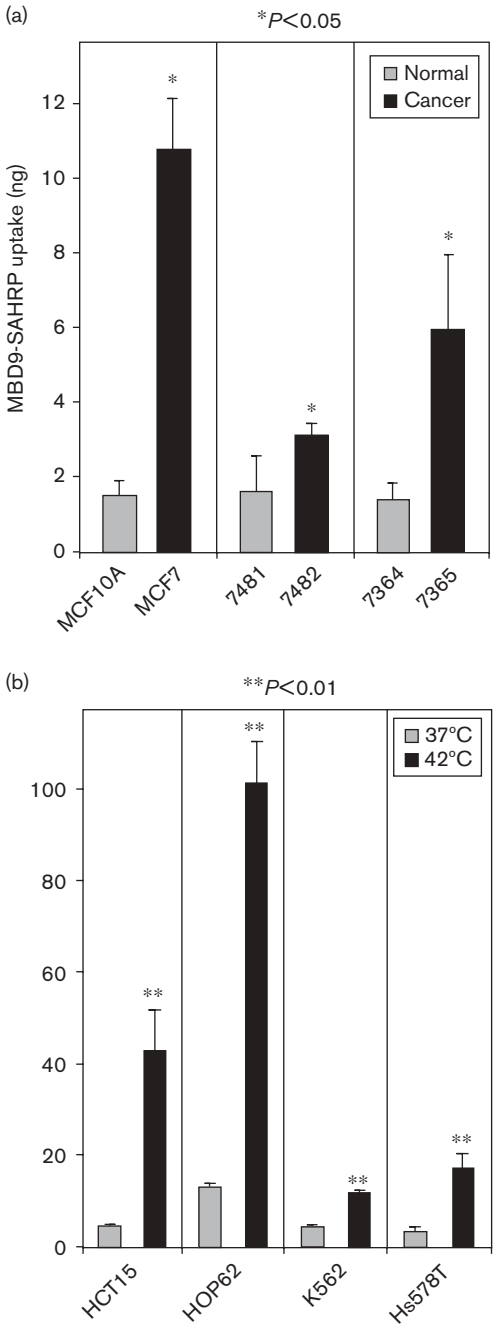

Uptake of metal-binding transporter domain (MBD)-tagged streptavidin–horseradish peroxidase complex (SAHRP) into cancer cells. Uptake of SAHRP was measured in cell lines as described in Methods. (a) Comparisons of uptake between paired cancer/noncancer cell lines. The cancer line in each pair is shown to the right. (b) The effect of heat shock on uptake. Uptake of SAHRP into cells grown at 37 or 42°C for 1 h was measured.

in cell culture by adding 100 ng/ml of MBD-tagged SAHRP to the culture medium. Of 54 cancer cell lines tested in this assay, most take up MBD-tagged SAHRP into cellular compartments efficiently (Table 1). On the basis of data from surface cross-linking studies performed using biotinylated MBD peptide in 48 of these same cell lines, MBD-SAHRP uptake correlates positively with surface markers previously implicated in MBD-mediated uptake: transferrin receptor, caveolin-1, and beta3-integrins (Table 2).

Table 2 Correlation of cross-linked surface markers to MBD-mediated uptake

	r
Transferrin receptor 1	0.377
Caveolin 1	0.338
Integrin α 2	NS
Integrin α 5	NS
Integrin α V	NS
Integrin α 6	NS
Integrin β 1	NS
Integrin β 3	0.304
Integrin β 5	NS

Only statistically significant ($P<0.05$) correlations are shown.
MBD, metal-binding transporter domain.

Gene array analysis and surface cross-linking studies reveal features of MBD-receptive cells pointing to their selectivity for uptake

Matched pairs of high-MBD-uptake and low-MBD-uptake cell lines (from seven different anatomical sites) were compared by gene array analysis. Maximally differentially expressed genes across the matched cell line pairs (5% most upregulated) showed that cell internalization of MBD-mobilized SAHRP in tumor cell lines is correlated with stress-response genes such as HSP70 and NF-κB. At least 80% of the upregulated genes play a role in cellular stress-coping mechanisms, whereas less than 10% of the downregulated genes do (Table 3). The gene most correlated with MBD uptake is GDF15, a member of the transforming growth factor-β family associated with cellular stress [23]. Extracellular GDF-15 levels were measured in a panel of 13 randomly selected cell lines (K562, HCT15, UO31, Hs578T, HOP62, HT29, NCI-H23, HCT116, A2780, PC3, A498, MCF7, and CCRF-CEM) and found to correlate closely with the previously measured levels of MBD-SAHRP uptake in these cell lines ($r = 0.76$). Cell stress such as heat shock also has a positive effect on cellular uptake of MBD-SAHRP (Fig. 1b).

Predicted and actual biodistribution of MBD-tagged peptides and proteins

GDF15 has previously been shown to be associated with malignancy in prostate cancer [24]. PCR analysis of a normalized human cDNA tissue panel (Clontech) using primers specific for GDF15, the gene most differentially upregulated in gene array analysis of high-MBD-uptake cell lines showed that placenta, kidney, and pancreas were particularly rich in GDF15 transcript. The biodistribution of MBD-tagged peptides (mice) and proteins

Table 3 MBD-uptake-related genes

Sprot/EMBL	Unigene	Ratio	Gene name
			Down-regulated genes
P08253	Hs.367877	0.035	MMP2: (MMP2 OR CLG4A) 72 KDA TYPE IV COLLAGENASE PRECURSOR
P35555	Hs.750	0.079	FIBRILLIN1: (FBN1 OR FBN) FIBRILLIN 1 PRECURSOR
Q15844	Hs.77274	0.135	UPA: (PLAU) UROKINASE-TYPE PLASMINOGEN ACTIVATOR PRECURSOR
P07996	Hs.164226	0.143	THROMBOSPONDIN1: (THBS1 OR TSP1 OR TSP)
P02462	Hs.437173	0.147	COL4A1: (COL4A1) COLLAGEN ALPHA 1(IV) CHAIN PRECURSOR
Q15579	Hs.169300	0.200	TGFB2: (TGFB2) TRANSFORMING GROWTH FACTOR BETA 2
P01584	Hs.126256	0.204	IL1B: (IL1B) INTERLEUKIN-1 BETA PRECURSOR (IL-1 BETA) (CATABOLIN)
P05121	Hs.414795	0.253	PAI1: (SERPINE1 OR PAI1) PLASMINOGEN ACTIVATOR INHIBITOR-1
P01009	Hs.297681	0.267	SERPINA1_1_HUMAN: (SERPINA1 OR AAT) ALPHA-1-ANTITRYPSIN PRE
Q14926	Hs.76753	0.276	ENG: (ENG OR END) ENDOGLIN PRECURSOR (CD105 ANTIGEN)
P05231	Hs.512234	0.288	IL6: (IL6 OR IFNB2 OR IL-6) INTERLEUKIN-6 PRECURSOR (IL-6)
Q9UE18	Hs.437536	0.289	LAMA4: (LAMA4) LAMININ ALPHA-4 CHAIN PRECURSOR
P10145	Hs.624	0.359	IL8_HUMAN: (IL8) INTERLEUKIN-8 PRECURSOR (IL-8) (CXCL8)
Q9BV78	Hs.252820	0.360	PLGF: (PGF OR PLGF) PLACENTA GROWTH FACTOR PRECURSOR
P55085	Hs.154299	0.380	PAR2: (PAR2 OR GPR11 OR F2RL1) PROTEINASE ACTIVATED RECEPTOR
P46013	Hs.80976	0.410	KI67: (MKI67) ANTIGEN KI-67
Q9Y2J6	Hs.194431	0.416	KIAA0992: (KIAA0992) KIAA0992 PROTEIN (FRAGMENT)
Q9ULV1	Hs.19545	0.422	FZD4: (FZD4) WNT RECEPTOR FRIZZLED-4
P07437	Hs.356729	0.439	TUBB1-TUBB5_HUMAN: (TUBB1) TUBULIN BETA-1 CHAIN
Q10718	Hs.2442	0.455	MDC9: (ADAM9 OR MDC9 OR KIAA0021 OR MLTNG)
			Up-regulated genes
O14629	Hs.296638	11.727	GDF15_2: (GDF15 OR PLAB) GROWTH/DIFFERENTIATION FACTOR 15
O60356	Hs.424279	3.848	P8: (P8 OR NUPR1 OR 2310032H04RIK) PROTEIN P8
P17066	Hs.3268	3.761	HSPA6-HSPA7: (HSPA6 OR HSP70B) HEAT SHOCK 70 KD PROTEIN 6/7
P22004	Hs.285671	2.843	BMP6: (BMP6 OR VGR1) BONE MORPHOGENETIC PROTEIN 6 PRE
Q9UPE2	Hs.126248	2.782	COL9A3: (COL9A3) ALPHA-3 TYPE IX COLLAGEN
Q9UQM0	Hs.274402	2.647	HSPA1A: (HSPA1A OR HSP70-1)
P05412	Hs.78465	2.349	JUN: (JUN) TRANSCRIPTION FACTOR AP-1 (ACTIVATOR PROTEIN 1)
P17275	Hs.400124	2.349	JUNB: (JUNB) TRANSCRIPTION FACTOR JUN-B (G0S3)
O75519	Hs.231975	2.280	CREM: (CREM) CAMP RESPONSIVE ELEMENT MODULATOR
P18847	Hs.460	2.156	ATF3: (ATF3) CYCLIC-AMP-DEPENDENT TRANSCRIPTION FACTOR ATF-3
P12931	Hs.436015	2.112	SRC: (SRC1) PROTO-ONCOGENE TYROSINE-PROTEIN KINASE SRC
Q9H4Z1	Hs.151738	2.079	MMP9: (MMP9 OR CLG4B) 92 KDA TYPE IV COLLAGENASE PRECURSOR
P10914	Hs.80645	2.063	IRF1: (IRF1) INTERFERON REGULATORY FACTOR 1 (IRF-1)
O95358	–	1.974	NSG-X_HUMAN: BRAIN AND NASOPHARYNGEAL CARCINOMA PROTEIN
Q9H4Z5	Hs.99029	1.969	CEBPB: (CEBPB OR TCF5) CCAAT/ENHANCER BINDING PROTEIN BETA
P35638	Hs.355867	1.965	GADD153: (DDIT3 OR CHOP) GROWTH ARREST AND DNA DAMAGE
P55327	Hs.2384	1.959	TPD52: (TPD52) TUMOR PROTEIN D52 (N8 PROTEIN) (MD52)
Q92473	Hs.26630	1.939	ABCA3: (ABCA3 OR ABC3) ATP-BINDING CASSETTE
Q16523	Hs.381081	1.900	PSMB9: (PSMB9 OR LMP2 OR RING12) PROTEASOME CHAIN 7 PRE
Q16202	Hs.193400	1.869	IL6R: (L6RA OR IL6R) INTERLEUKIN-6 RECEPTOR ALPHA CHAIN PRE

MBD, metal-binding transporter domain.

(rats) favors kidney and pancreas (Fig. 2) suggesting the possibility of using MBD-based delivery for organ-biased treatment of malignancies and recurrent metastatic disease.

MBD-tagged peptides exhibit broad-spectrum cytoxicity to cancer cells in cell culture

A test collection of MBD-tagged peptides designed to inhibit various stress-coping mechanisms was synthesized, based on published peptide sequence data (Table 4). Furthermore, as shown in the case of PEP1, MBD is more efficient at promoting cellular uptake than the widely used antennapedia transporter module; based on the MBD sequence scaffold, single-residue substitution mutants of PEP1 with higher specific activities can be selected (Table 5). Alanine scanning of a different class of MBD-tagged peptides (MDOKSH) was undertaken as a further illustration of site-specific optimization: 48 mutants were synthesized, purified, and tested in CCRF-CEM and MCF-7. The cytotoxicity of the 48 variant peptides was strongly correlated in the two cell line assay systems ($r = 0.606$). Mutant 27 exhibits greatly enhanced cytotoxicity in both cell line assays (Table 6). Finally, as summarized in Table 7, MBD-tagged peptides targeting stress-coping and anti-apoptotic mechanisms are cytotoxic to a broad range of cancer cell lines from a variety of anatomical sites.

MBD-tagged peptides chemosensitize breast cancer cells to 5-fluorouracil

Two MBD-tagged peptides, PEP2 and CSK41, were added to cultured cells to test their cytotoxic effects alone and in combination with marginally effective doses of 5-FU. To test specificity for cancer cells, cytotoxicity assays were carried out in paired normal/cancer breast cell line pairs (CRL7481/CRL7482, CRL7364/CRL7365, and MCF10A/MCF7). PEP2 and CSK41 added in a 1 : 1 ratio (by weight) at 0, 3.125, 6.25, 12.5, and 25.0 μg/ml revealed significant differences in cytotoxicity against

Fig. 2

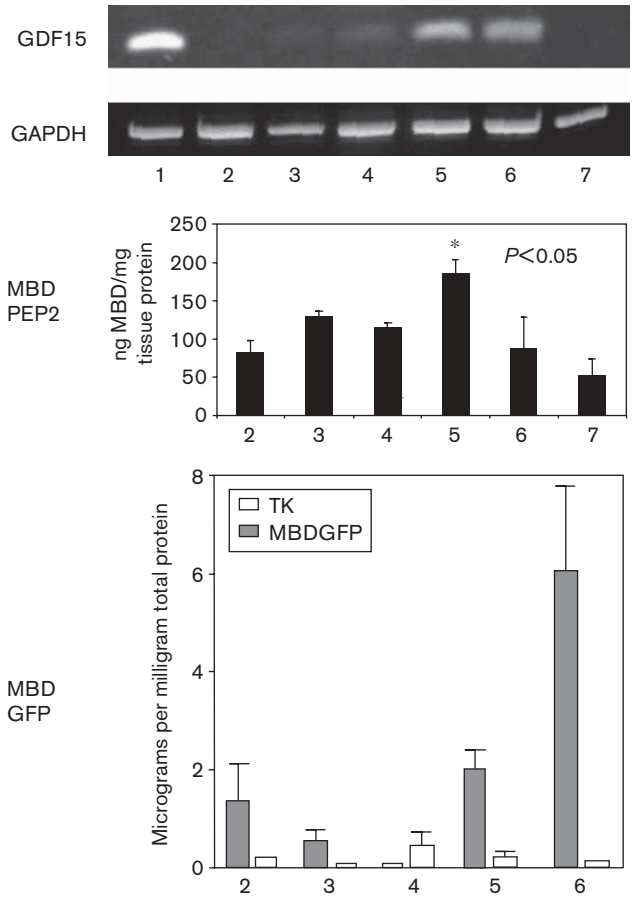

Biodistribution of metal-binding transporter domain (MBD)-tagged molecules. Top panel: PCR analysis of standardized tissue cDNAs was performed as described in Methods. GAPDH primers were used as controls. 1, placenta; 2, heart; 3, lung; 4, liver; 5, kidney; 6, pancreas; 7, peripheral blood cells. Middle panel: Three Balb/c mice received a single subcutaneous bolus injection of 2 mg/kg PEP2 peptide (Table 1) and tissue extracts were prepared at 2 h postinjection. An MBD-specific antibody was used to measure peptide concentrations in tissues by enzyme-linked immunosorbent assay. Tissue legend as in the top panel. Lower panel: Six rats received a single subcutaneous bolus injection of 2 mg/kg MBD-tagged GFP protein [20] and thymidine kinase (TK) protein as a control. Tissue extracts were prepared at 2 h postinjection. GFP and TK immunoreactivity in tissues was measured by ELISA. Tissue legend as in the top panel.

Table 4 MBD-tagged cytotoxic peptide sequences

Peptide	# AA	Sequence	Reference
MBD-SMZ	22	KKGFYKKKQCRPSKGRKRGFCW	TW
MBD9	26	KKGFYKKKQCRPSKGRKRGFCWNGRK	1
MBD21	28	KKGFYKKKQCRPSKGRKRGFCWAVD KYG	1
PNC-28	27	ETFSDLWKLLKK*WKMRRNQFWVKVQRG*	42
NFKB	34	KKGFYKKKQCRPSKGRKRGFC WAPVQRKRQKLMP	38
NEMO	34	KKGFYKKKQCRPSKGRKRGFC WAALDWSWLQT	39
VIVIT	35	KKGFYKKKQCRPSKGRKRGFCWGPHP VIVITGPHE	40
MDOKSH	31	KKGFYKKKQCRPSKGRKRGFCWKPLYW DLYE	46
MDOKSH27	31	KKGFYKKKQCRPSKGRKRGFCWAPLYW DLYE	TW
NPKC	38	AKKGFYKKKQCRPSKGRKRGFCWPSI QITSLNPEWNET	44
P38	39	AKKGFYKKKQCRPSKGRKRGFCWAPS RKPALRVIIPQAGK	45
PEP1	32	ETFSDLWKLLKKGFYKKKQCRPSKGRKR GFCW	TW
PEP2	32	ETFSDVWKLLKKGFYKKKQCRPSKGRKR GFCW	TW
PEP3	32	ETFSDIWKLLKKG- FYKKKQCRPSKGRKRGFCW	TW
CSK	34	KKGFYKKKQCRPSKGRKRGFCWA VAEYARVQKRK	41
CSK41	40	AVAEYAWVQKRKG- FYKKKQCRPSKGRKRGFCKALYWDLYE	TW
HSBP1	42	KKGFYKKKQCRPSKGRKRGFCWAR IDDMSSRIDDLEKNIADL	47
HSBP2	42	KKGFYKKKQCRPSKGRKRGFCWAVQ TLLQQMQDKFQTMSDQI	47
MSURVN	43	AKPFYKKKGFYKKKQCRPSKGRKRG FCWGSSGLGEFLKLDRER	43
MDOKB3	33	KKGFYKKKQCRPSKGRKRGFCW PYTLLRRYGRD	TW

MBD, metal-binding transporter domain; TW, this work.

Table 5 MBD-tagged cytotoxic peptides: cytotoxicity of MBD versus antennapedia domain

Peptide	MDA-MB-231	MX-1	Hs578T
MBD9	100.0 ± 1.1	100.0 ± 5.5	100.0 ± 6.2
PNC-28	74.7 ± 5.8*	50.2 ± 4.8*	70.6 ± 5.6*
PEP1	64.9 ± 7.9*	15.4 ± 2.1*,**	37.7 ± 1.3*,**
PEP2	40.7 ± 1.8*,***	6.8 ± 1.5*,***	33.5 ± 2.3*,***
PEP3	32.9 ± 1.7*,***	9.0 ± 0.6*,***	33.2 ± 0.7*,***

Forty-eight-hour cell survival is shown for three breast cancer lines treated with 25 μg/ml peptide.
MBD, metal-binding transporter domain.
*$P<0.01$ vs. MDB9; **$P<0.01$ vs. PNC-28; ***$P<0.01$ vs. PEP1.

cancer versus normal cells as well as a strong additive effect with marginally effective concentrations of 5-fluorouracil (Fig. 3).

Use of MBD-tagged peptides in animal models

Intracardial injection of human HL-60 leukemia cells into Rag-2 mice generates high levels of human cell circulation in the PB, mimicking leukemia [25,26]. This Rag-2 mouse model was used to test other leukemia cell lines (RPMI-8226, MOLT-4, CCRF-CEM). Intracardial injection of CCRF-CEM, a T-cell leukemia line, resulted in efficient establishment of systemic disease in PB and organs within 7 days and caused splenomegaly and death in the animals by day 21. Similar progression of disease was seen using MOLT-4 or RPMI-8226 but symptoms were less severe and slower to develop (not shown). The efficacy of an MBD-tagged peptide cocktail was tested using CCRF-CEM in this model. By genomic DNA PCR using human-specific primers (100 ng/rxn, 25 cycles) on spleens collected after a 7-day treatment with 4 mg/kg MBD-peptide cocktail consisting of equal parts by weight of PEP2, CSK, MDOKB3, and MDOKSH peptides (16 days total), a significant reduction in CCRF-CEM

cell count was observed, compared with the saline-treated controls. Splenomegaly was also reduced significantly in animals injected with MBD peptide versus animals injected with saline. In the bone marrow of these animals the reduction in human cell burden did not reach significance ($P = 0.068$). However, when MDA-MB-435 was used in this model instead of CCRF-CEM (Fig. 4), the reduction in bone marrow burden with peptide treatment was statistically significant ($P = 0.039$).

Table 6 MBD-tagged cytotoxic peptides: alanine scan of MDOKSH peptide

		Cell survival[a]	
Peptide	Sequence	CCRF-CEM	MCF-7
MDOKSH	KKGFYKKKQCRPSKGRKRG FCWKPLYWDLYE	100	100
Mutant 6	KKGFYKKKQCRPSKGRKRG FCWKPLYWDLYEI	62.3 ± 5.0	68.5 ± 6.5
Mutant 9	KKGFYKKKQCRPSKGRKRG FCWKPLYWDLYEM	63.8 ± 4.6	56.8 ± 8.1
Mutant 11	KKGFYKKKQCRPSKGRKRG FCWKPLYWDLYEP	64.8 ± 7.2	59.6 ± 10.7
Mutant 23	KKGFYKKKQCRPSKGRKRG FCWKPLYWALYE	74.5 ± 8.0	58.8 ± 8.1
Mutant 27	KKGFYKKKQCRPSKGRKRG FCWKALYWDLYE	41.0 ± 5.1	38.8 ± 7.5
Mutant 28	KKGFYKKKQCRPSKGRKRG FCWAPLYWDLYE	60.1 ± 11.1	52.7 ± 11.7
Mutant 48	AKGFYKKKQCRPSKGRKR GFCWKPLYWDLYE	71.8 ± 10.7	61.6 ± 3.1

[a]Expressed relative to the activity of the parental peptide MDOKSH.
MBD, metal-binding transporter domain.

Fig. 3

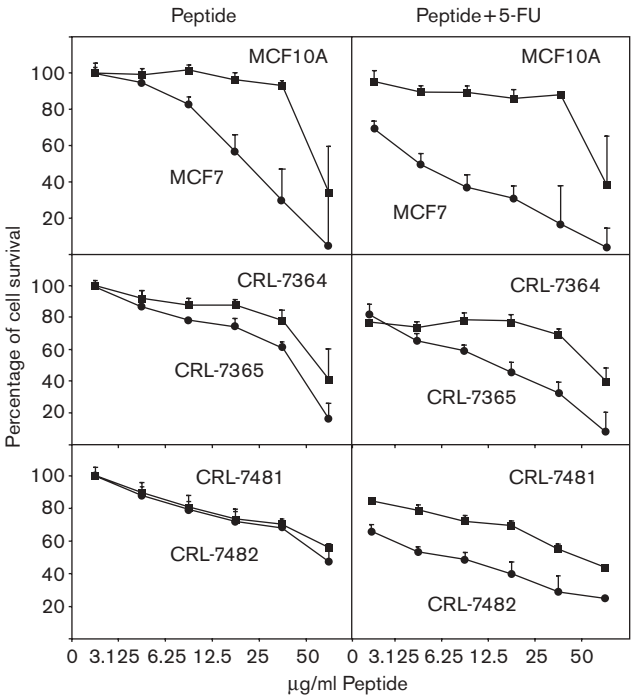

Selective chemosensitization of cancer cell lines. Cell survival after 48-h treatment with the indicated concentrations of peptide (PEP2 + CSK41, 1 : 1 by weight) was measured as described in Methods. For each line the marginal dose of 5-fluorouracil (5-FU) that produced 20% cell death was established in preliminary experiments and used in the experiments shown in the right side panels. Each panel shows survival curves for paired cancer/normal cell lines.

Table 7 Cytotoxicity of MBD therapeutic peptides

	Leukemia line (% viability @ 48 h/25 μg/ml peptide)				Breast cancer line (% viability @ 48 h/25 μg/ml peptide)				
Peptide	CCRF-CEM	MOLT-4	SR	RPMI-8826	MCF-7	MDA-MB231	MDA-MB435	Hx578T	MX-1
CSK	75.1 ± 4.5	81.0 ± 7.1			21.1 ± 4.1			50.2 ± 1.6	
	85.5 ± 2.3	54.8 ± 9.7			41.3 ± 5.8			76.3 ± 0.6	
NFKB	47.4 ± 13.9	35.9 ± 6.8		64.6 ± 14.3	32.8 ± 17.7	91.6 ± 6.1	18.0 ± 1.6	36.3 ± 5.6	74.1 ± 6.1
		22.5 ± 3.5					29.6 ± 2.6	30.6 ± 2.7	
NEMO			56.9 ± 6.2		77.0 ± 46.7	79.0 ± 0.8	67.4 ± 21.1	81.3 ± 3.0	59.1 ± 3.2
							90.2 ± 3.6		
VIVIT	72.1 ± 9.2	35.2 ± 4.3	63.3 ± 10.3	59.8 ± 19.2					
HSBP1					77.1 ± 20.3			77.7 ± 5.2	
HSBP2	92.6 ± 2.0				94.2 ± 17.1		88.9 ± 4.0	81.7 ± 2.9	
							87.7 ± 6.7		
PEP2	71.7 ± 10.0	63.5 ± 7.7	33.7 ± 16.0	38.4 ± 4.2	19.3 ± 6.3	40.7 ± 1.8	18.5 ± 1.0	31.1 ± 3.0	6.8 ± 1.5
	5.9 ± 2.6	57.9 ± 1.3			33.5 ± 4.4			33.5 ± 2.3	9.0 ± 0.6
	80.0 ± 14.6	88.2 ± 2.6			35.6 ± 5.7				
PEP3	86.8 ± 3.1	73.0 ± 5.5	75.9 ± 15.7		27.5 ± 15.2	32.9 ± 1.7	16.0 ± 2.0	18.6 ± 1.7	
	24.5 ± 8.3	58.3 ± 16.5			30.6 ± 5.7		27.0 ± 3.9	55.1 ± 4.1	
	82.4 ± 7.1				21.7 ± 1.5			33.2 ± 0.7	
MSURVN					52.3 ± 3.5	91.4 ± 3.3	93.8 ± 1.8	77.2 ± 4.7	
					64.7 ± 5.0		86.0 ± 2.2		
MDOKB3					92.4 ± 5.4		74.5 ± 1.8	77.6 ± 5.6	
					82.0 ± 5.9		80.7 ± 22.8		
MDOKSH	52.4 ± 12.6				72.1 ± 8.2				
	79.8 ± 3.7								
	73.7 ± 12.7								

Percent cell viabilities that were significantly lower ($P < 0.05$) relative to control cells treated with an equal dose of control MBD peptide are shown (data from one to four representative experiments).
MBD, metal-binding transporter domain.

Fig. 4

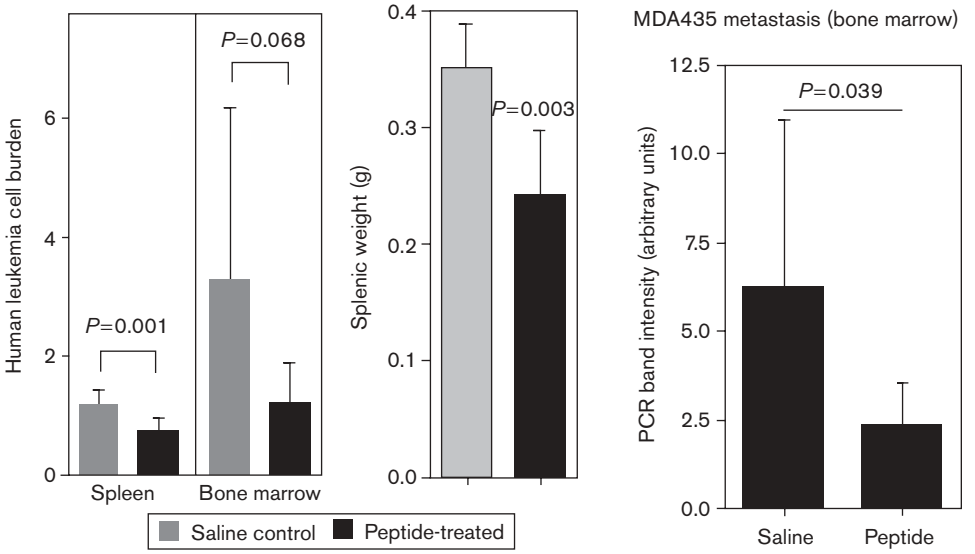

Effect of metal-binding transporter domain (MBD)-tagged cytotoxic peptides in animal models of human cancer. Left panel: PCR using human-specific primers was performed on 500 ng genomic DNA extracted from tissues collected from CCRF-CEM-injected Rag-2 mice (six to 10 animals per group) to detect leukemia cell burden in bone marrow and spleen. Spleen weights are shown on the right side of the left panel. Right panel: PCR analysis of genomic DNA extracted from bone marrow from MDA-MB-435-injected Rag-2 mice (saline $n=8$, peptide $n=10$).

Discussion

The overall purpose of this study was to develop targeted biological modifier therapies for disseminated disease and to characterize their selectivity. In this work, we show that MBD transporter-tagged peptides can be effectively delivered to cancer cells, both *in vitro* and *in vivo*. The cytotoxicity of these peptides seemed to be highly selective for cancer cells, when compared with normal cell counterparts. In the Rag-2 model of disseminated disease MBD-tagged peptides reduced CCRF-CEM human leukemia cell burden in spleen and splenomegaly. When MDA-MB-435 cells were used instead of CCRF-CEM, MBD-tagged peptides significantly reduced human cell burden in the bone marrow. Taken together, our results suggest that a multifactorial approach to disseminated disease can incorporate multiple elements of designed specificity at the levels of cellular uptake (MBD) and mechanistic toxicity, that is, targeting pathways specifically upregulated in cancer cells. We further demonstrate synergy between MBD-tagged cytotoxic peptides and low-level 5-FU to achieve chemosensitization. The goal is to target cellular fragilities peculiar to proliferative disease with high specificity to sensitize such cells and increase the effectiveness of adjuvant chemotherapies, in effect enhancing patient quality of life by allowing lower doses of the latter to be used.

Specificity in systemic cancer therapy can be conceptually considered at a number of levels beyond monoclonal antibody-based homing to a target, a method used successfully by earlier investigators, notably using the erbB2 receptor [27]. We set out to investigate targeted delivery based on MBD-specified selective uptake of a therapeutic molecule by cancer cells, as well as mechanistic selectivity of the agent inside the cell. We have shown proof-of-principle in both cases. In this work, selective uptake of MBD by cancer cells has been demonstrated. Furthermore, fusion of MBD to previously described sequences that were shown by others to be selectively active against mechanisms of particular importance to cancer cells [14,15,28–35] results in the creation of peptide molecules with a broad spectrum of activity against cancer cells and selective cytotoxicity against the cancerous counterpart of cancer–normal cell pairs. We have also shown proof-of-principle that the cytotoxicity of MBD-tagged peptides can be elevated by conventional alanine-scanning techniques.

Broad spectrum of action is of particular relevance to a field wherein variability between cancer types and between individual patients is substantial. In this respect it is worth noting that some MBD-tagged cytotoxic peptides show a large spectrum of activity across numerous cell lines from a variety of anatomical sites.

The mechanistic underpinnings for the ability of the MBD transporter to selectively specify internalization into cancer cells was extensively investigated in this work. Gene arrays revealed a strong correlation between

MBD uptake and the expression of genes (such as GDF15), which are known to be associated with injury and stress. The cell surface markers transferrin receptor, caveolin, and integrin-β-3 were found to correlate with MBD uptake. A previous study [20] had implicated these molecules mechanistically in MBD (and, presumably, in IGFBP-3) uptake. The sequences of the peptides MBD9 and MBD21 differ slightly in that the latter contains a putative caveolin-binding site [20]. In this work, we show that the ability of these two peptides to specify cellular uptake does vary across a large panel of cancer cell lines, perhaps because of this difference.

A practical consideration in the design of new biological agents is whether they are compatible with existing chemotherapeutic agents widely used in clinical settings. One such agent is 5-FU (and modern counterparts such as capecitabine), which is relatively inexpensive and widely prescribed for a broad range of cancers. In this work, we show an additive effect between MBD-tagged cytotoxic peptides and marginal doses of 5-FU, when tested against cancer cells but not against their 'normal' cell counterparts. The possible clinical relevance of such an observation lies in the possibility of using lower doses of 5-FU clinically without loss of effectiveness against cancer cells but with reduced side effect profiles.

Breast cancer metastasis to bone is a frequent and painful complication of the primary neoplastic event. The stromal environment of bone is essential for successful outgrowth of metastatic cells in that environment [36]. It has been suggested that this is because some stromal factors regulating normal mammary development (e.g. metalloproteinase 9, WNT-1, IGF-1) are also known to regulate bone development [37–39]. The bone marrow environment also provides fatty tissue and rich vasculature, similar to breast tissue [40], which may furnish an attractive environment for migrating breast cancer cells.

The ability to access privileged sites such as bone marrow is a promising characteristic of MBD-tagged therapeutic molecules. In this work, we have used the intrinsic transporter characteristics of the MBD domain to deliver designed peptide sequences to cancer cells. Unlike traditional biologics, such as monoclonal antibodies, a feature of MBD-based approaches is that delivery of the therapeutic molecule occurs into (rather than onto) cells, allowing a rich diversity of intracellular molecules to be targeted, at least in principle.

Although MBD is a natural domain of IGFBP-3, a moderately abundant human protein in circulation, immunological methods using anti-MBD polyclonal antibodies fail to detect this domain in plasma and even in highly purified IGFBP-3 itself unless the domain is unmasked by treatment with ferrous (but not ferric) ions [20]. It is thus unlikely that the use of the MBD domain as a transporter *in vivo* will be confounded by the presence of endogenous IGFBP-3.

With regard to stability, solubility, and other practical characteristics that might affect their use as therapeutic molecules, MBD-tagged peptides exhibit more favorable profiles than conventional biologics based on larger proteins (our unpublished observations). In addition to simplicity and lower cost of manufacturing, they also offer, in principle, additional options for transdermal, intra-nasal, and implant-based delivery not generally available to larger molecules.

Future approaches might conceivably use a combination of the homing characteristics of monoclonal-antibody-based technologies with the cellular-uptake and intracellular mechanistic specificities of MBD-tagged molecules that we demonstrate in this work. It may be worth noting in this context that MBD-tagged antibodies can themselves also be effectively internalized by cells *in vitro* (unpublished observations), suggesting yet additional possibilities.

References

1 Nylandsted J, Brand K, Jaattela M. Heat shock protein 70 is required for the survival of cancer cells. *Ann N Y Acad Sci* 2000; **926**:122–125.
2 Nylandsted J, Wick W, Hirt UA, Brand K, Rohde M, Leist M, *et al.* Eradication of glioblastoma, and breast and colon carcinoma xenografts by Hsp70 depletion. *Cancer Res* 2002; **62**:7139–7142.
3 Hortobagyi GN. Treatment of breast cancer. *N Engl J Med* 1998; **339**:974–984.
4 Chong YP, Mulhern TD, Cheng HC. C-terminal Src kinase (CSK) and CSK-homologous kinase (CHK) – endogenous negative regulators of Src-family protein kinases. *Growth Factors* 2005; **23**:233–244.
5 Rao RD, Mladek AC, Lamont JD, Goble JM, Erlichman C, James CD, Sarkaria JN. Disruption of parallel and converging signaling pathways contributes to the synergistic antitumor effects of simultaneous mTOR and EGFR inhibition in GBM cells. *Neoplasia* 2005; **7**:921–929.
6 Nebbioso A, Clarke N, Voltz E, Germain E, Ambrosino C, Bontempo P, *et al.* Tumor-selective action of HDAC inhibitors involves TRAIL induction in acute myeloid leukemia cells. *Nat Med* 2005; **11**:77–84.
7 Ciocca DR, Clark GM, Tandon AK, Fuqua SA, Welch WJ, McGuire WL. Heat shock protein hsp70 in patients with axillary lymph node-negative breast cancer: prognostic implications. *J Natl Cancer Inst* 1993; **85**:570–574.
8 Cornford PA, Dodson AR, Parsons KF, Desmond AD, Woolfenden A, Fordham M, *et al.* Heat shock protein expression independently predicts clinical outcome in prostate cancer. *Cancer Res* 2000; **60**:7099–7105.
9 Strik HM, Weller M, Frank B, Hermisson M, Deininger MH, Dichgans J, *et al.* Heat shock protein expression in human gliomas. *Anticancer Res* 2000; **20**:4457–4462.
10 Ricaniadis N, Kataki A, Agnantis N, Androulakis G, Karakousis CP. Long-term prognostic significance of HSP-70, c-myc and HLA-DR expression in patients with malignant melanoma. *Eur J Surg Oncol* 2001; **27**:88–93.
11 Ciocca DR, Vargas-Roig LM. Hsp27 as a prognostic and predictive factor in cancer. *Prog Mol Subcell Biol* 2002; **28**:205–218.
12 Li GC, Hahn GM. Interactions of hyperthermia and drugs: treatments and probes. *Natl Cancer Inst Monogr* 1982; **61**:317–323.
13 Volloch V, Sherman MY. Oncogenic properties of Hsp72. *Oncogene* 1999; **18**:3648–3651.
14 Lin YZ, Yao SY, Veach RA, Torgerson TR, Hawiger J. Inhibition of nuclear translocation of transcription factor NF-kappa B by a synthetic peptide containing a cell membrane-permeable motif and nuclear localization sequence. *J Biol Chem* 1995; **270**:14255–14258.
15 May MJ, D'Acquisto F, Madge LA, Glöckner J, Pober JS, Ghosh S. Selective inhibition of NF-kappaB activation by a peptide that blocks the interaction of NEMO with the IkappaB kinase complex. *Science* 2000; **289**:1550–1554.

16 Njemini Ambrosini G, Adida C, Altieri DC. A novel anti-apoptosis gene, survivin, expressed in cancer and lymphoma. *Nat Med* 1997; **3**:917–921.
17 Li F, Ackermann EJ, Bennett CF, Rothermel AL, Plescia J, Tognin S, *et al*. Pleiotropic cell-division defects and apoptosis induced by interference with survivin function. *Nat Cell Biol* 1999; **1**:461–466.
18 Midgley CA, Desterro JM, Saville MK, Howard S, Sparks A, Hay RT, Lane DP. An N-terminal p14ARF peptide blocks Mdm2-dependent ubiquitination in vitro and can activate p53 in vivo. *Oncogene* 2000; **19**:2312–2323.
19 Zhang R, Mayhood T, Lipari P, Wang Y, Durkin J, Syto R, *et al*. Fluorescence polarization assay and inhibitor design for MDM2/p53 interaction. *Anal Biochem* 2004; **331**:138–146.
20 Singh BK, Charkowicz DA, Mascarenhas DD. IGF-independent effects mediated by a C-terminal metal-binding domain of insulin-like growth factor binding protein-3. *J Biol Chem* 2004; **279**:477–487.
21 Chicha L, Tussiwand R, Traggiai E, Mazzucchelli L, Bronz L, Piffaretti JC, *et al*. Human adaptive immune system Rag2-/-gamma(c)-/- mice. *Ann N Y Acad Sci* 2005; **1044**:236–243.
22 Matsuda H, Seo Y, Kakizaki E, Kozawa S, Muraoka E, Yukawa N. Identification of DNA of human origin based on amplification of human-specific mitochondrial cytochrome region. *Forensic Sci Int* 2004; **152**:109–114.
23 Zimmers TA, Jin X, Hsiao EC, McGrath SA, Esquela AF, Koniaris LG. Growth differentiation factor-15/macrophage inhibitory cytokine-1 induction after kidney and lung injury. *Shock* 2005; **23**:543–548.
24 Cheung PK, Woolcock B, Adomat H, Sutcliffe M, Bainbridge TC, Jones EC, *et al*. Protein profiling of microdissected prostate tissue links growth differentiation factor 15 to prostate carcinogenesis. *Cancer Res* 2004; **64**:5929–5933.
25 De Lord C, Clutterbuck R, Titley J, Ormerod M, Gordon-Smith T, Millar J, *et al*. Growth of primary human acute leukemia in severe combined immunodeficient mice. *Exp Hematol* 1991; **19**:991–993.
26 Paine-Murrieta GD, Taylor CW, Curtis RA, Lopez MHA, Dorr RT, Johnson CS, *et al*. Human tumor models in the severe combined immune deficient (scid) mouse. *Cancer Chemother Pharmacol* 1997; **40**:209–214.
27 Whenham N, D'Hondt V, Piccart MJ. HER2-positive breast cancer: from trastuzumab to innovatory anti-HER2 strategies. *Clin Breast Cancer* 2008; **8**:38–49.
28 Aramburu J, Yaffe MB, López-Rodríguez C, Cantley LC, Hogan PG, Rao A. Affinity-driven peptide selection of an NFAT inhibitor more selective than cyclosporin A. *Science* 1999; **285**:2129–2133.
29 Takayanagi H, Juji T, Miyazaki T, Iizuka H, Takahashi T, Isshiki M, *et al*. Suppression of arthritic bone destruction by adenovirus-mediated csk gene transfer to synoviocytes and osteoclasts. *J Clin Invest* 1999; **104**:137–146.
30 Picksley SM, Vojtesek B, Sparks A, Lane DP. Immunochemical analysis of the interaction of p53 with MDM2: fine mapping of the MDM2 binding site on p53 using synthetic peptides. *Oncogene* 1994; **9**:2523–2529.
31 Sun C, Nettesheim D, Liu Z, Olejniczak ET. Solution structure of human survivin and its binding interface with Smac/Diablo. *Biochemistry* 2005; **44**:11–17.
32 Ron D, Luo J, Mochly-Rosen D. C2 region-derived peptides inhibit translocation and function of beta protein kinase C in vivo. *J Biol Chem* 1995; **270**:24180–24187.
33 Barsyte-Lovejoy D, Galanis A, Sharrocks AD. Specificity determinants in MAPK signaling to transcription factors. *J Biol Chem* 2002; **277**: 9896–9903.
34 Ling Y, Maile LA, Badley-Clarke J, Clemmons DR. DOK1 mediates SHP-2 binding to the alphaVbeta3 integrin and thereby regulates insulin-like growth factor I signaling in cultured vascular smooth muscle cells. *J Biol Chem* 2005; **280**:3151–3158.
35 Tai LJ, McFall SM, Huang K, Demeler B, Fox SG, Brubaker K, *et al*. Structure-function analysis of the heat shock factor-binding protein reveals a protein composed solely of a highly conserved and dynamic coiled-coil trimerization domain. *J Biol Chem* 2002; **277**:735–745.
36 Moreau JE, Anderson K, Mauney JR, Nguyen T, Kaplan DL, Rosenblatt M. Tissue-engineered bone serves as a target for metastasis of human breast cancer in a mouse model. *Cancer Res* 2007; **67**:10304–10308.
37 Smid M, Wang Y, Klijn JGM, Sieuwerts AM, Zhang Y, Atkins D, *et al*. Genes associated with breast cancer metastasizing to bone. *J Clin Oncol* 2006; **24**:2261–2267.
38 Curran S, Murray GI. Matrix metalloproteinases in tumour invasion and metastasis. *J Pathol* 1999; **189**:300–308.
39 Fong YC, Maa MC, Tsai FJ, Chen WC, Lin JG, Jeng LB, *et al*. Osteoblast-derived TGF-beta1 stimulates IL-8 release via AP-1 and NF-kappaB in human cancer cells. *J Bone Miner Res* 2008; **23**:961–970.
40 Paget S. The distribution of secondary growths in cancer of the breast. *Cancer Metastasis Rev* 1989; **8**:98–101.